Magnetic aging in TiO2-doped Mn-Zn ferrites

Magnetic Aging in TiO_2-doped Mn-Zn Ferrites

Cinzia Beatrice[1*], Samuel Dobák [1,2], Vasiliki Tsakaloudi[3], Fausto Fiorillo[1], Alexandra Manioudaki[3] and Vassilios Zaspalis[3,4]

[1]Advanced Material Metrology and Life Science Division, Istituto Nazionale di Ricerca Metrologica, 10135 Torino, Italy

[2]Institute of Physics, Faculty of Science, P.J. Šafárik University, 04154 Košice, Slovakia

[3]Laboratory of Inorganic Materials, Chemical Process and Energy Resources Institute, Centre for Research and Technology Hellas, 57001 Thermi-Thessaloniki

[4]Laboratory of Materials Technology, Department of Chemical Engineering, Aristotle University of Thessaloniki, 54124 Thessaloniki, Greece

ABSTRACT

The soft magnetic properties of the Mn-Zn ferrites can be stabilized versus changing temperature by addition of CoO in suitable proportion. The material benefits in this case of anisotropy compensation brought about by the Co^{2+} cations. However, prolonged exposure of magnetic cores to high temperatures, as likely to occur in automotive applications, can be associated with local phenomena of induced anisotropy, resulting in magnetic viscosity and aging. We show in this paper that proper addition of TiO_2 in optimally CoO-doped ferrites can restrain aging and the ensuing detrimental effects on loss of permeability. Experiments have been performed, at 23 °C and 100 °C, across the broad frequency and peak polarization ranges, DC–1 GHz and 2 mT - 200 mT, respectively, on 3000 ppm CoO-doped Mn-Zn ferrite ring samples, prepared by conventional ceramic processing. It is shown that 5000 ppm TiO_2 doped ferrites subjected to a 100-hour treatment at 200 °C show minor deterioration of their soft magnetic properties, compared with the conventional ferrites containing 1000 ppm TiO_2. We demonstrate that this effect chiefly relates to a correspondingly reduced value of the magnetic anisotropy induced by directional ordering at 200 °C, a result apparently related to diffusion hindering of the Co^{2+} cations by the dissolved Ti^{4+} cations. The induced anisotropy, however, while leading to increased hysteresis and excess losses, brings about a decrease of the rotational loss at intermediate frequencies.

Keywords—Mn-Zn ferrites, magnetic losses, magnetic aging, magnetic anisotropy.

* Corresponding author: c.beatrice@inrim.it

I. INTRODUCTION

Increasing demand for loss reduction in inductive components for power electronics calls for efficient and temperature stable Mn-Zn ferrite cores. The magnetic properties of Mn-Zn ferrites are actually tailored to some extent by calibrated additions of oxides, which can either modify microstructure and grain growth, segregate at the grain boundaries, or, by dissolving in the lattice, modify the intrinsic physical and magnetic properties of the cores [1-3]. CoO, in particular, is known to mitigate the usually strong dependence of energy loss and permeability on temperature via the mechanism of anisotropy compensation, where the Co^{2+} cations introduce a positive term, partly countering the native negative magnetocrystalline anisotropy constant of the host lattice [4 - 7]. This can be proved by directly estimating the average value of the temperature-dependent effective anisotropy constant $<K_{eff}>$, a feat made possible by the determination of the dc rotational permeability [8, 9]. It shows that optimal compensation is achieved for CoO = 3000 – 4000 ppm. However, at sufficiently high temperatures the Co^{2+} ions will tend to diffuse and preferentially populate the B-sites along the <111> axes lying closer to the local magnetization, in order to attain a lower energy configuration (directional ordering). Unequal distribution of the Co^{2+} ions among the four <111> axes will arise, resulting in induced uniaxial anisotropy in each domain and inside each domain wall (dw), parallel or nearly parallel to the local magnetization direction. This configuration, frozen up upon cooling, will cause an increase of the macroscopic anisotropy, besides creating potential wells at the positions occupied by the dws. The ensuing degradation of core loss and permeability is unwelcome, especially for the Co-doped ferrites used in high-quality inductor cores for automotive applications.

It was shown in the past that the presence of Ti^{4+} ions in Co-doped Mn-Zn ferrites remarkably increases the long-term stability of core loss and permeability, because Ti^{4+} ions hinder the diffusion and directional ordering of the Co^{2+} ions [10]. The mechanism by which this occurs is possibly related to the formation of tightly bound Ti^{4+}-Fe^{2+} pairs and ensuing suppression of electron hopping between Fe^{2+} and Fe^{3+} ions [11]. It is known in fact that such electron displacement is instrumental in weakening the potential that the Co^{2+} must overcome in order to diffuse [12].

In the present work we investigate the magnetic loss and permeability behaviors (DC – 1 GHz, 0 °C – 130 °C) at different values of the peak polarization J_p (2 mT – 200 mT) in CoO = 3000 ppm doped Mn-Zn ferrites, where either 1000 ppm or 5000 ppm TiO_2 additions are made. The measurements are made before and after a 100-hour aging treatment at 200 °C. By singling out the rotational permeability, we calculate the effective average anisotropy constant $<K_{eff}>$ and we find that its increase with aging goes hand in hand with general deterioration of the soft magnetic properties, namely the increase of the dw-related hysteresis W_h and excess $W_{exc}(f)$ loss components and the associated decrease of the permeability at all J_p values. The restraining action on aging by the soluted Ti^{4+} ions is, however, apparent when passing from the 1000 ppm to the 5000 ppm TiO_2 addition. This is especially appreciated in the upper J_p range, beyond some 20 – 50 mT, where the contribution $J_{p,dw}$ by the dws to J_p becomes important. The theory shows, in any case, and the experiments confirm that at frequencies ranging between some 100 kHz and 2 MHz, the energy loss can actually decrease, depending on the J_p value, upon aging. This depends on the proportion between $J_{p,dw}$ and $J_{p,rot}$ and the related loss contributions. As discussed in the following, the rotational loss $W_{rot}(f)$, which is associated with spin damping and the related resonant energy absorption, unfolds according to the spectral

distribution of the ferromagnetic resonance frequencies, that is, of the anisotropy fields. It happens then that any treatment, like aging, modifying such a distribution will predictably affect the dissipation by spin damping.

II. EXPERIMENTAL PROCEDURE

Mn-Zn ferrites were prepared by the conventional method of solid-state processing, based on the chemical formula $[Mn_{0.83}\ Zn_{0.16}\ Co_{0.001}]\ Fe_{1.90}\ O_4$. High-purity raw materials (all provided by Merck, Analytical Grade) were weighed, mixed and prefired at 850 °C in air. The prefired mixtures were doped following a fixed doping scheme for broad temperature range power applications that includes CaO and Nb_2O_5 additions, while Ti-doping varied between 1000 and 5000 ppm. The doped powders were milled for 9 hours using water as a dispersion medium. Drying of the milled slurry and roll granulation of the ferrite powder was performed using 0.2 wt.% Polyvinyl Alcohol (Merck, Analytical Grade, MW72000) as a binder. Toroidal specimens of 14 mm outside diameter were uniaxially compacted to a press density of 2.90 ± 0.02 g/cm^3. Sintering of the compacted specimens was performed at 1325 °C, following a controlled partial oxygen pressure profile, according to the Morineau-Paulus equilibrium. The sinter density of the specimens was measured by the Archimedes' method. The morphological characteristics of the prepared powders were evaluated by particle size distribution (Malvern Mastersizer S) and pore size distribution (Quantachrom). The structural characteristics were examined by X-Ray Diffraction. The polycrystalline microstructure of the sintered specimens was investigated by Scanning Electron Microscopy (SEM, JEOL 6300), after grinding, polishing and chemical etching of the sintered, pure, and aged Mn-Zn ferrite cores. Image processing on the obtained SEM data was performed using AnalySIS Soft Imaging System (Olympus). Selected sintered toroids of each synthesis with Ti variation were aged by exposure to an aging treatment at 200 °C for 100 hours in air. Selected samples were also thinned by grinding, from the as-obtained ~ 5 mm thickness to a final ~ 1 mm thickness, in order to assess the role of eddy currents in the measured high-frequency losses.

The magnetic characterization was performed on the ferrite ring samples (outside diameter $D_{ext} = 14$ mm, inside diameter $D_{int} = 9$ mm) by fluxmetric measurements at defined peak polarization J_p ($2\ \text{mT} \le J_p \le 200\ \text{mT}$) from quasi-static (200 Hz) up to 10 MHz versus frequency using a calibrated hysteresisgraph-wattmeter. A transmission line (TL) method using a Vector Network Analyzer (VNA Rohde & Schwarz ZNB8) on a short-circuited coaxial line was instead adopted in the frequency range $100\ \text{kHz} \le f \le 1\ \text{GHz}$ to measure the complex permeability via the reflection scattering parameter S_{11}. A transmission electromagnetic wave power $P_{TL} = 10$ mW was used. On approaching the MHz frequency region the power limitations of the fluxmetric setup impose restraints on the magnetic characterization with values of $J_p \ge 50$ mT. The corresponding loss figure nevertheless can be extrapolated to the VNA high-frequency measurements (see the continuous lines in Fig. 2). Assuming quasi-linear response of the material, the measured high-frequency real μ' and imaginary μ'' permeability components are independent of P_{TL} (i.e. J_p) and one obtains the energy loss at a given J_p value as

$$W(J_p, f) = \pi J_p^2 \mu''(f) / [\mu'^2(f) + \mu''^2(f)] \qquad [\text{J/m}^3]. \tag{1}$$

The saturation polarization J_s was obtained by measuring the upper portion of the magnetization curve, up to applied field H of few kA/m, and extrapolating J vs. $1/H \to 0$. Measurements above room temperature were made by keeping the sample inside a nylon cell endowed with a dc-supplied non-inductive heater and by detecting the sample temperature by means of a copper-constantan micro-thermocouple stuck on the sample surface. A detailed

discussion on the magnetic measurement method and the way the VNA results under given PTL are reconciled with the fluxmetric measurements made at given J_p is provided in [13, 14].

III. BASIC STRUCTURAL AND MAGNETIC PROPERTIES

The investigation of the polycrystalline microstructure of the Mn-Zn ferrite cores, as presented in Fig. 1, showed that regular grain growth occurred in all samples before the aging treatment and revealed a homogeneous polycrystalline microstructure. Uniform grain size distribution was observed by the SEM images of the sintered specimens, with the average grain diameter slightly decreasing, from 11.80 μm to 10.07 μm, when increasing the TiO_2 content from 1000 to 5000 ppm, in agreement with previous literature results [15]. Little or no defects were detected before aging, whereas the aged ferrite samples showed intergranular imperfections, such as sub-grain boundaries and cavities, as revealed after standard chemical etching. Such imperfections are more frequent in the 5000 ppm TiO_2-doped ferrite core.

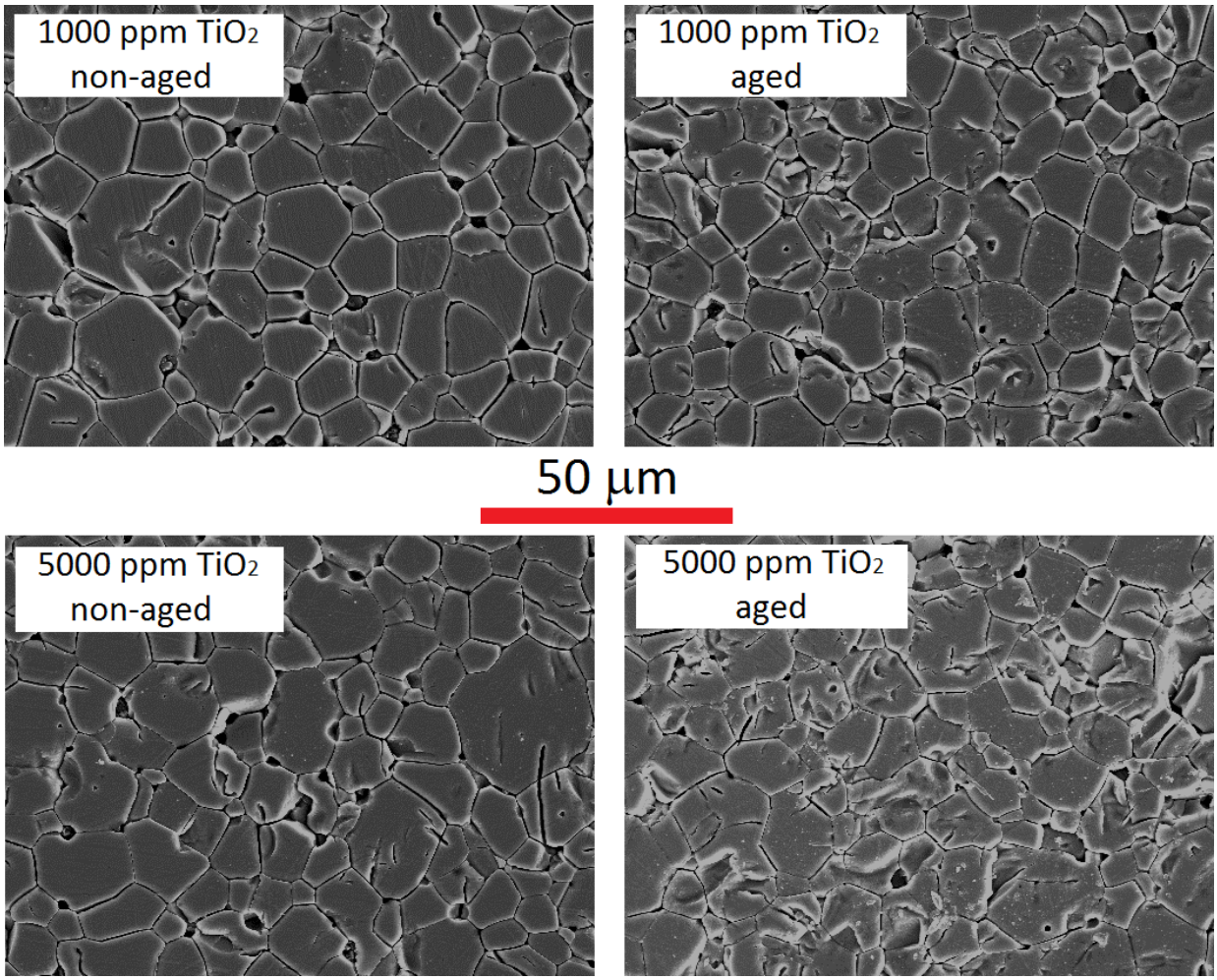

Fig. 1. SEM micrographs of CoO = 3000 ppm doped Mn-Zn ferrite samples, with either 1000 ppm or 5000 ppm TiO_2 additions, sintered at 1325 °C. Intergranular imperfections appear after the 100-hour aging at 200 °C.

Complete broadband magnetic characterization at selected J_p values from 2 mT up to 200 mT was performed on the ring samples both at room temperature and at T = 100 °C. Fig. 2 provides an example of the loss $W(f)$ measured at 100 °C, before and after aging, in the 1000 ppm and 5000 ppm TiO_2 ferrites. The symbols provide the $W(f)$ values obtained by the fluxmetric measurements, the continuous lines, overlapping with the fluxmetric results at intermediate frequencies, are the result of the transmission line method. A number of features emerge from these two examples. First, aging always engenders an increase of the low-frequency loss (i.e., up to about 100 kHz), more remarkable in the 1000 ppm TiO_2 ferrite beyond some 20 mT. Second, a wide region at intermediate frequencies appears where $W(f)$ decreases after aging, a somewhat unusual result. Third, the loss is quite independent of aging at upper frequencies, beyond a few MHz. To note that this turns out to be the sole region where eddy current losses can be appreciated, at least in the present 5 mm thick or possibly thicker samples. They disappear, in any case, in

sufficiently thin (e.g. ~ 1 mm) specimens. We can see in Fig. 3 that aging of the quasi-static (hysteresis) loss W_h is more effective with increasing J_p, that is, with the increase of the dw proportion $J_{p,dw}$ /$J_{p,rot}$. The increase of W_h has a counterpart in the associated decrease of the dc permeability, with the important difference that, while the dw displacements are the sole responsible for the effect of aging on W_h, the rotations play a basic role on the behavior of the permeability on soft ferrites. This is highlighted by the example of measured real permeability $\mu'(f, J_p)$ shown in Fig. 4. The permeability decomposition $\mu'(f, J_p) = \mu'_{rot}(f) + \mu'_{dw}(f, J_p)$ is here brought to light, making use of a simple iterative method for singling out the rotational contribution $\mu'_{rot}(f)$. This method, fully discussed in [16], is based on the idea that the quasi static imaginary permeability is exclusively associated with the dws ($\mu''_{dc}(J_p) = \mu''_{dc,dw}(J_p)$) and that $\mu'_{rot}(f)$ is independent of J_p up to about 50-100 mT, an acceptable approximation in typical Mn-Zn ferrites. It is understood in Fig. 4 that $J_{p,rot}$ provides a fundamental contribution at all frequencies. It actually becomes the sole contribution on entering the MHz range, following the relaxation of the dw processes. It is also apparent in Fig. 4 that the maximum decrease of the permeability due to aging occurs in the low frequency range, whereas, as already guessed from the behavior of $W(f)$ in Fig. 2, negligible effects are observed beyond a few MHz. Looking then at dc permeability μ_{dc}, we observe in Fig. 5 the beneficial role of 5000 ppmTiO_2 addition, by which the decrease of μ_{dc} ensuing from the 100-hour aging treatment is limited to about 10 %.

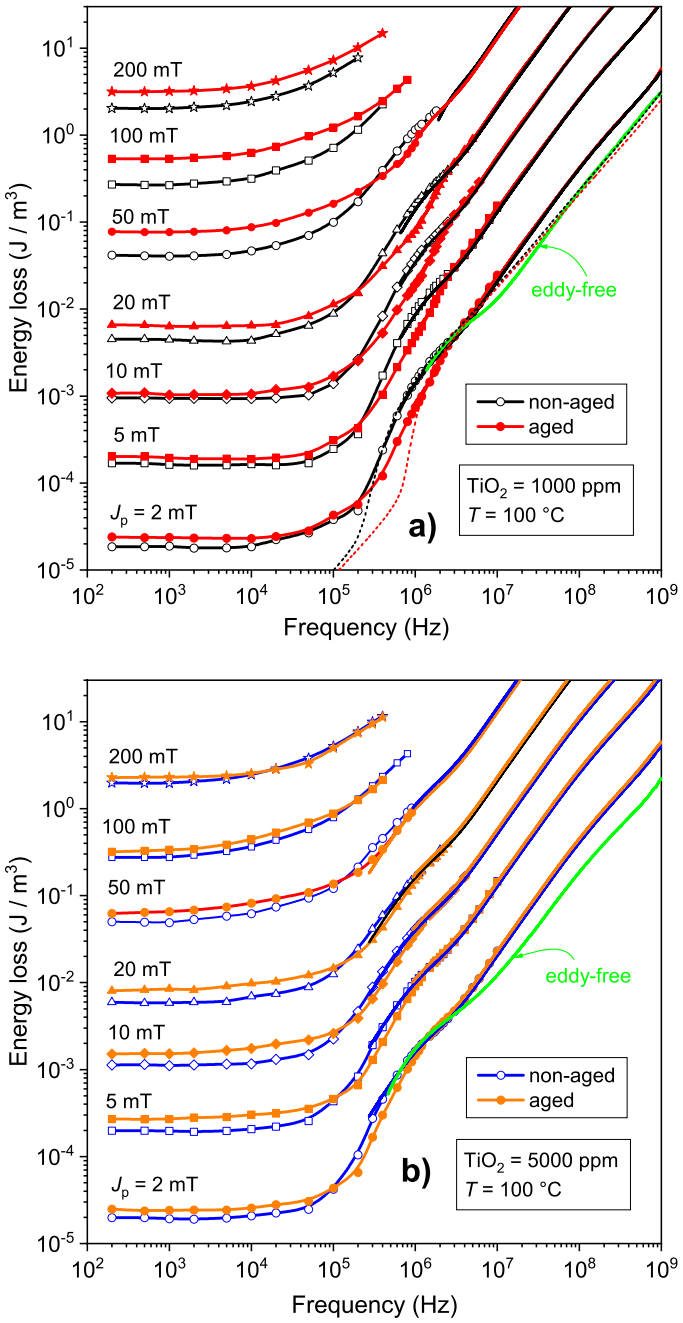

Fig. 2. Broadband behavior of the magnetic loss $W(f)$ measured between 2 mT and 200 mT in the CoO = 3000 ppm doped Mn-Zn ferrites before and after the aging treatment. Symbols and continuous lines provide the $W(f)$ values obtained by the fluxmetric and transmission line method, respectively. The results shown in (a) are obtained for low (1000 ppm) TiO_2 addition. High TiO_2 content (5000 ppm) modifies the response to aging as in (b). $W(f)$ displays, depending on the J_p value, somewhat opposite trends upon TiO_2 addition in the low and intermediate frequency ranges. The eddy current free $W(f)$ curve is obtained on a 1mm thick sample. The short-dash lines in Fig. 2a provide an example of prediction of the rotational loss component $W_{rot}(f)$.

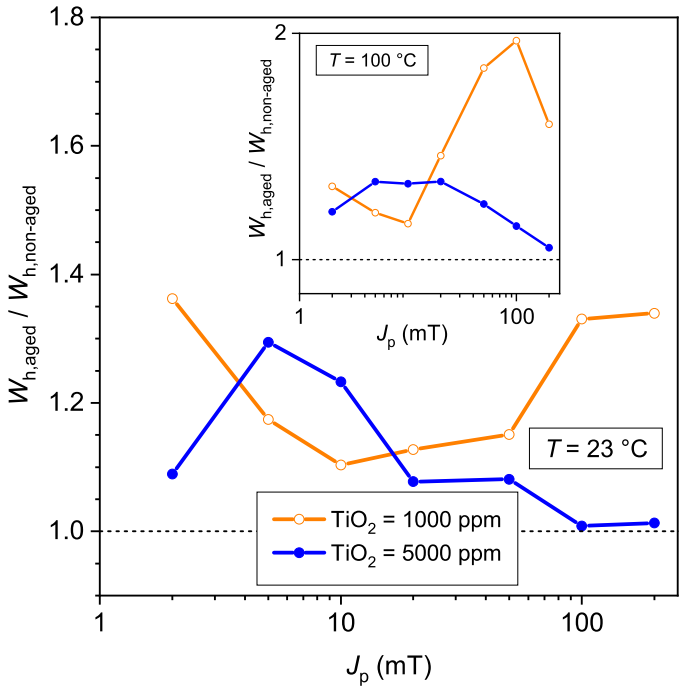

Fig. 3. Aged versus non-aged quasi-static loss $W_{h,aged}$ / $W_{h,non-aged}$ at room temperature and at 100 °C as a function of peak polarization in the 1000 ppm and 5000 ppm TiO_2 enriched ferrites. Higher concentration of Ti^{4+} ions is conducive the major restraint of aging in the upper J_p range, concurrent with an increasing proportion of the domain wall contribution J_{pdw}.

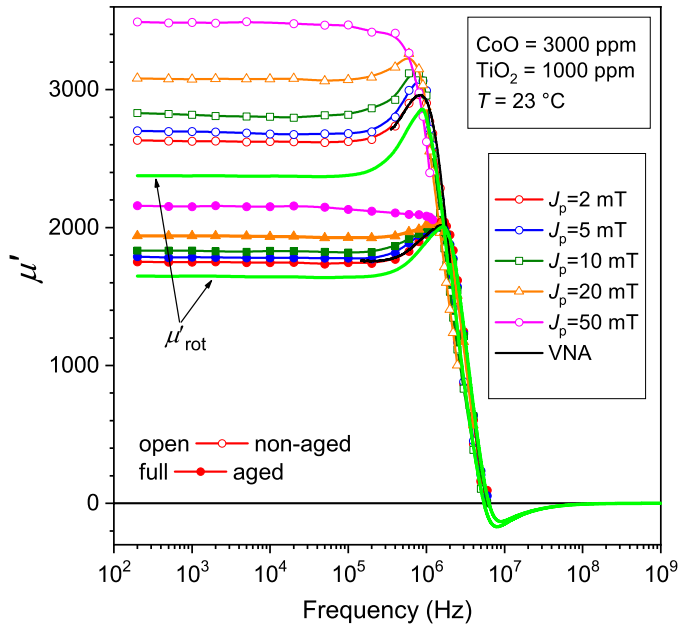

Fig. 4. Effect of aging on the real permeability component and its dependence on frequency at room temperature in the 1000 ppm TiO_2 ferrite. The rotational contribution $\mu'_{rot}(f)$, independent of J_p, is singled out (continuous lines). Both μ'_{rot} and the dw contribution $\mu'_{dw}(f, J_p) = \mu'(f, J_p) - \mu'_{rot}(f)$ are depressed by the aging treatment. To note the stronger effect suffered by $\mu'_{dw}(f, J_p)$ and the coalescence of the $\mu'(f, J_p)$ curves in the upper frequency range, where only rotations survive.

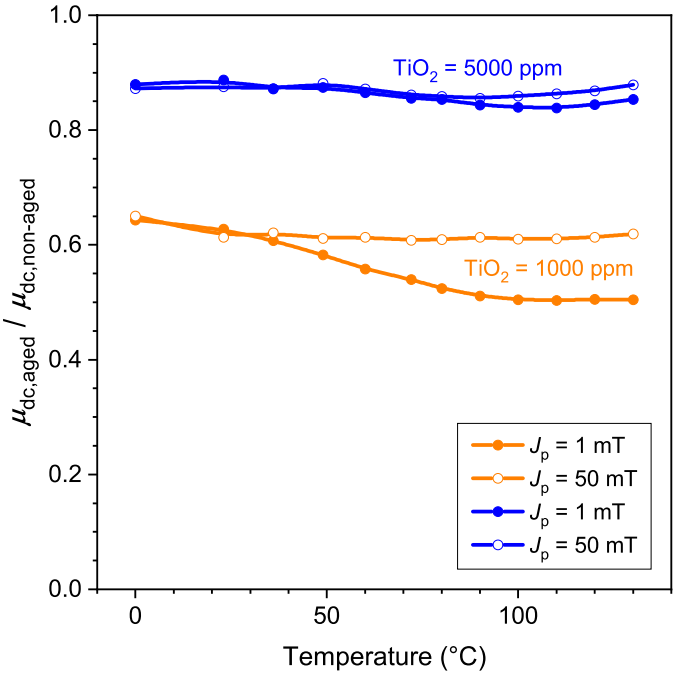

Fig. 5. Ratio $\mu_{dc,aged}$ / $\mu_{dc,non\text{-}aged}$ of the quasi-static permeabilities at J_p = 1 mT and J_p = 50 mT before and after the aging treatment and its dependence on temperature. To note that at 1 mT $J_p \sim J_{p,rot}$.

IV. MAGNETIC LOSSES AND AGING: A COHERENT INTERPRETATIVE APPROACH

The complex phenomenology sketched in Figs. 2-5 descends from the interplay of the dw and rotational processes and the way they contribute to the macroscopic magnetic response of the ferrite as a function of J_p, f, $<K_{eff}>$, T, and the material microstructural properties. By recognizing the nature of these two magnetization mechanisms, for example, the fact that the dws tend to relax their motion with increasing frequencies, while the rotations respond to the ac field by precession around the local easy axis and undergo resonant-dissipative behavior at the frequency dictated by the local anisotropy field, we subject them to appropriate separate theoretical treatment. We have shown in Fig. 4 an example providing separate $\mu'_{rot}(f)$ and, implicitly, $\mu'_{dw}(f, J_p)$. By knowledge of $\mu'_{rot,dc} \cong \mu_{rot,dc}$ we get breakthrough information, that is, an estimate of $<K_{eff}>$ at any temperature. In fact, under the assumption of uniform distribution of the orientation of the easy axes, we predict

$$< K_{eff}(T) > \cong \frac{J_s^2(T)}{3\mu_0 \mu_{rot,dc}(T)}, \qquad (2)$$

where μ_0 is the magnetic constant and J_s is the saturation polarization. J_s is measured to vary between 0.524 T and 0.503 T at room temperature on passing from the 1000 ppm to 5000 ppm TiO_2 and to decrease at T = 130 °C to 0.368 T and 0.343 T, respectively. It is then understood that a main result of the extra-addition of TiO_2 is the clear limitation of the increase of the average effective anisotropy in the aged ferrites, as illustrated by the calculated dependence of $<K_{eff}>$ versus T shown in Fig. 6. The concurrent behaviors of the measured hysteresis loss W_h at J_p = 50 mT, shown in the inset of Fig. 6, confirm the role of high TiO_2 content on curbing the effect of aging. Under quite general terms, we can write the hysteresis loss as

$$W_h(J_p) = 8a(J_p)\sqrt{A}\frac{\sqrt{<K_{eff}>}}{J_s<s>} \cdot \frac{\mu_{dw,dc}}{\mu_{dw,dc}+\mu_{rot,dc}} J_p \ , \qquad (3)$$

where $a(J_p)$ is a suitable coefficient, taking into account the existence of a distribution of the local coercive fields and the microstructural details of the dw pinning centers, A is the exchange stiffness constant and $<s>$ is the average

grain size. By Eq. (3) we predict the presence of a minimum in the $W_h(J_p)$ vs. T dependence, basically related to the behavior of the $\frac{\sqrt{<K_{eff}>}}{J_s}$ ratio. The dashed lines shown in the inset of Fig. 6, calculated by Eq. (3) with defined value of the parameter $a(J_p)$, tend to underestimate the increase of $W_h(J_p)$ at low temperatures, reflecting the complexity of the dw processes. For example, the stabilization of the walls by directional ordering of the Co^{2+} cations during aging does introduce an extra potential well for the dws, that is, an extra barrier to be overcome (viscosity field) for their motion. This adds to the description descending from Eq. (3). Such a situation is clearly one occurring in the aged 1000 ppm TiO_2 ferrites, as put in evidence by the constricted shape of the hysteresis loop (see Fig. 7).

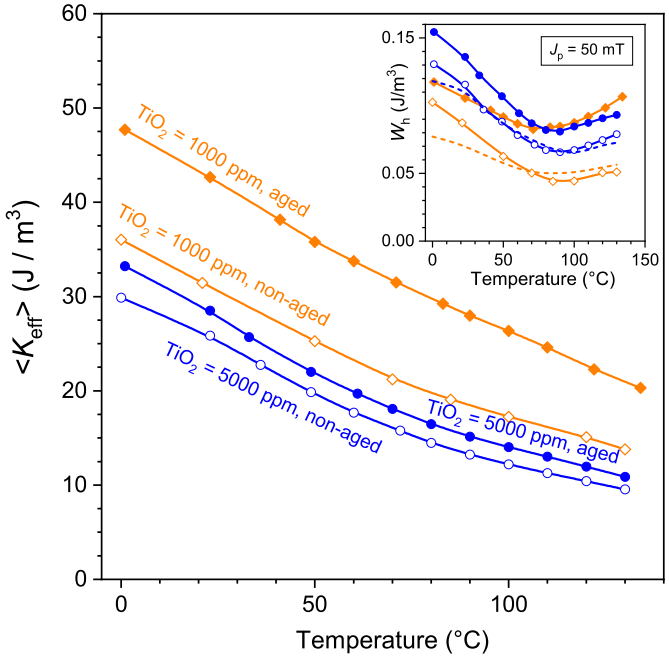

Fig. 6. Effective anisotropy $<K_{eff}>$ versus temperature before and after the aging treatment. The restrained increase of $<K_{eff}>$ in the high-TiO_2 ferrite is apparent. The inset shows the corresponding behavior of the hysteresis loss W_h, whose increase with aging is similarly mitigated. The dashed lines are calculated by Eq. (3), with constant value of $a(J_p)$.

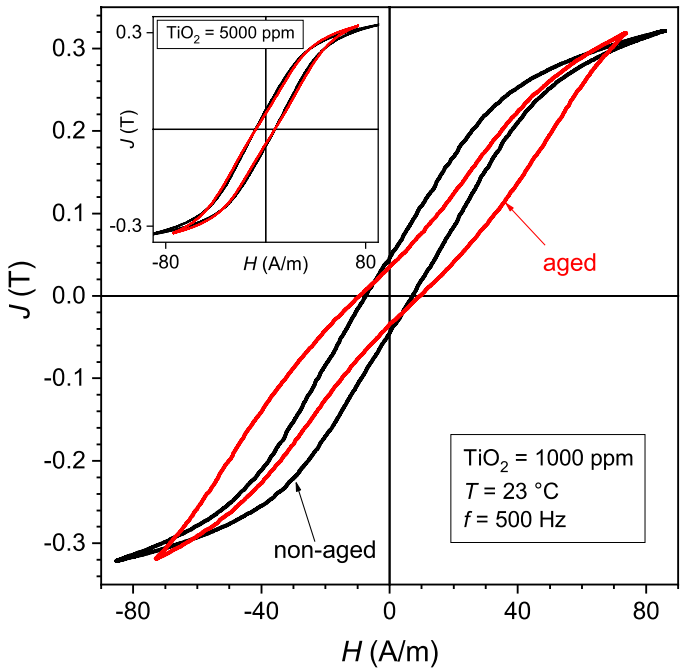

Fig. 7. Quasi-static hysteresis loops in the aged and non-aged Mn-Zn ferrites with low and high TiO_2 content. The constricted shape of the loop in the aged 1000 ppm TiO_2 ferrite puts in evidence the stabilization of the domain walls in their potential well, resulting from the Co^{2+} directional ordering occurring inside the wall. This effect is greatly restricted in the 5000 ppm TiO_2 ferrites, as shown in the inset.

The separation between the dw and rotational magnetization processes, of which Fig. 4 provides an example, is the starting point for the analysis of the magnetic losses as a function of frequency. In treating the $W(f)$ behavior we need to rely on such a separation and take at face value the different nature of the dynamics of dws and rotating spins in the bulk, the first displaying a dissipative response localized at the wall position and having a relaxation character, the second being endowed with resonant behavior and much larger spatial resolution, say of the order of the grain size. As discussed in previous works [9, 16], we can decompose the dw contribution into a quasi-static hysteresis W_h and a dynamic excess $W_{exc}(f)$ component, following the Statistical Theory of Losses and its extension to non-conducting magnetic materials [17, 18], and, because of the direct relationship between complex permeability and energy loss, as quantified by Eq. (1), it is natural to try to predict the rotational loss by predicting μ'_{rot} and μ''_{rot}. This is indeed possible, because the rotational response to the ac field can be described through the Landau-Lifshitz-Gilbert (LLG) equation, which provides a solution for the real χ'_{rot} and imaginary χ''_{rot} rotational susceptibilities for any domain subjected to the local effective anisotropy field $H_{k,eff}$ [13]. This quantity is obviously distributed in strength and orientation. We have shown that a log-normal distribution function $g(H_{k,eff})$ for the amplitude of $H_{k,eff}$ can excellently compare with the experiments

$$g(H_{k,eff}) = \frac{1}{\sqrt{2\pi}\sigma(H_{k,eff}-H_{k0})} \exp\left\{-\frac{[\ln(H_{k,eff}-H_{k0})-h]^2}{2\sigma^2}\right\}, \quad (4)$$

where $h = <\ln(H_{k,eff})>$, σ is the standard deviation of $\ln(H_{k,eff})$, and H_{k0} is the lower threshold of $H_{k,eff}$. It is remarked that on attaining frequencies deep in the MHz range an increasing number of grains, having overcome the local resonance condition, depending on the local $H_{k,eff}$, become magnetically transparent and do not compensate for the

internal magnetostatic fields. This implies that $g(H_{k,eff})$ tends to drift towards higher $H_{k,eff}$ values, an effect which is accounted for by h increasing with frequency as

$$h(f) = < \ln\left(H_{k,eff}^{(dc)} + C\,\frac{1-\frac{|\chi(f)|}{\chi_{dc}}}{1+|\chi(f)|} \right) >, \qquad (5)$$

with C a constant. By integrating over $g(H_{k,eff})$ and assuming an isotropic angular distribution of the easy axes, we eventually predict the macroscopic permeability components $\mu'_{rot}(f) = 1 + < \chi'_{rot}(f) >$ and $\mu''_{rot}(f) = < \chi''_{rot}(f) >$. An example of so-obtained prediction of $\mu'_{rot}(f)$ and $\mu''_{rot}(f)$ is given in Fig. 8 (dashed lines) for the 1000 TiO_2 ferrite. To remark here how dc value and resonance region move in accordance with the average value $<H_{k,eff}>$. This quantity is actually found to vary between 135 and 206 A/m at 23 °C and between 87 and 147 A/m at 100 °C. Having calculated the rotational permeability, it is an easy matter to obtain the rotational loss by means of Eq. (1), now written as $W_{rot}(f) = \pi J_p^2(f)\,\frac{\mu''_{rot}(f)}{|\mu(f)|^2}$. An example of calculated $W_{rot}(f)$ is shown in Fig. 9 (dashed lines). The calculation refers to the eddy current free thin ($d \sim 1$ mm) sample. Incidentally, this measurement permits us to verify that the eddy current loss at high frequencies is consistent with the equation for the classical loss

$$W_{cl,eddy}(J_p, f) = \left(\frac{\pi^2}{6}\right)\sigma'(f)\cdot(12k(R)S)J_p^2 f \quad , \qquad [J/m^3] \qquad (6)$$

where $\sigma'(f)$ is the real part of the measured conductivity and $k(R)$ is an increasing function of the aspect ratio R of the cross-section of area S. It is given by $k(R) = 0.0744R - 0.0434R^2$. But a further important result of the theoretical prediction, already anticipated in Fig. 2a, is brought to light in Fig. 9b, where the softer, non-aged ferrite, endowed with lower $<H_{k,eff}>$ value, exhibits higher rotational losses at intermediate frequencies. The higher $<H_{k,eff}>$ the higher the frequencies at which resonance and the related energy absorption come into play. From this viewpoint, aging favorably affects $W(f)$. The intersection of the $W(f)$ curves in Fig. 2 finds here a clear explanation. It is further noted in Fig. 9b how by restraining aging we also restrain this effect.

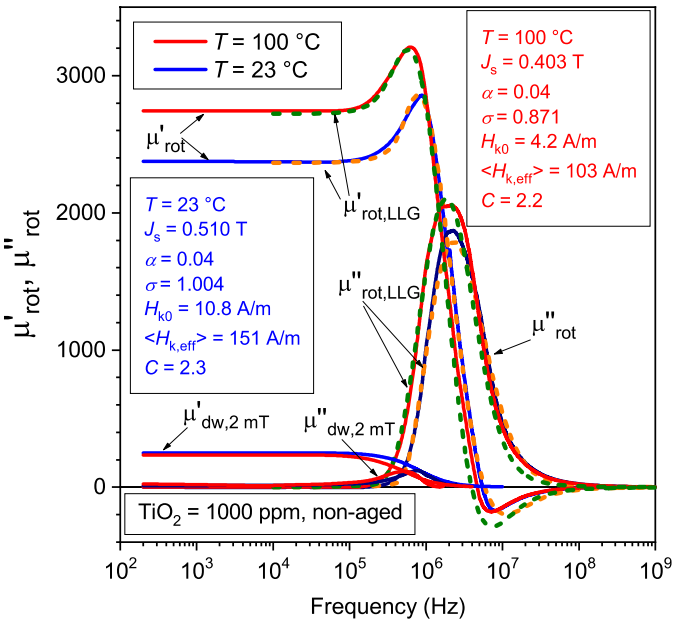

Fig. 8. Example of real and imaginary rotational permeability components and their frequency dependence at two temperatures. The dashed lines represent their fitting via the Landau-Lifshitz-Gilbert equation and use of the distribution function $g(H_{k,eff})$ (Eq. (4)) for the effective anisotropy field. α is the damping constant, σ is the width of the log-normal distribution, H_{k0} is the lower limit for the effective anisotropy field $H_{k,eff}$ and C is a parameter regulating the evolution of $g(H_{k,eff})$ at very high frequencies.

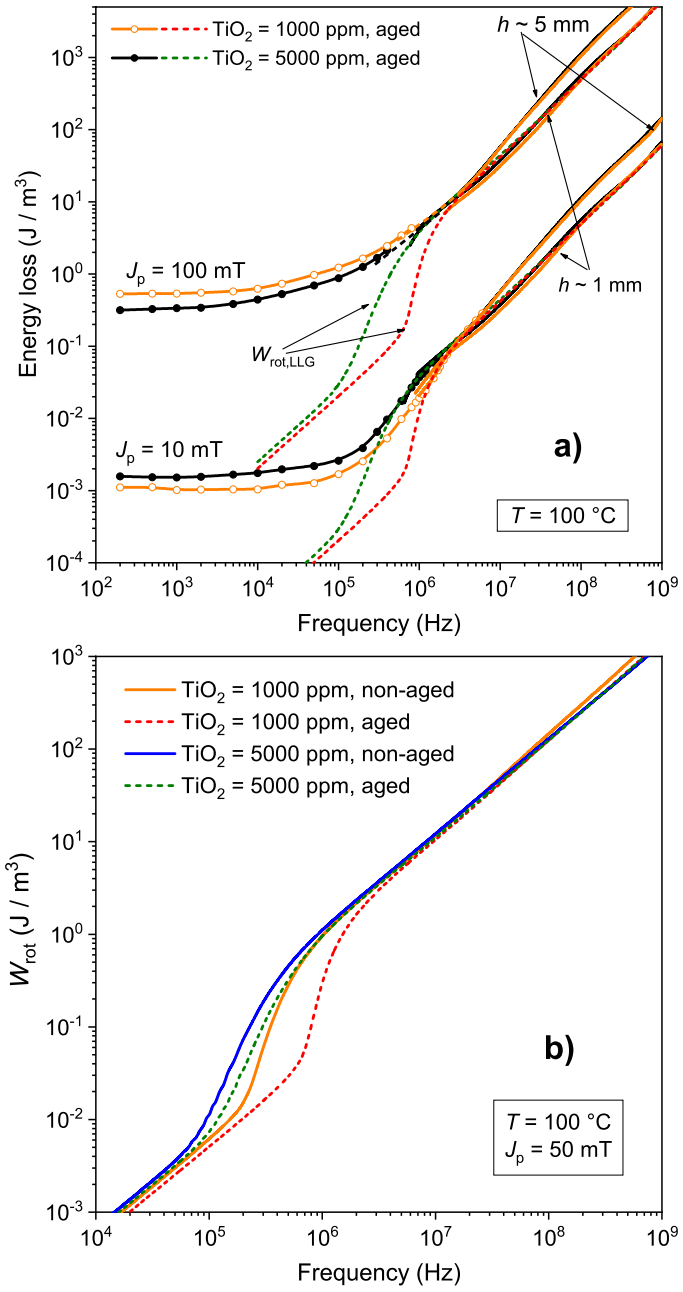

Fig. 9. a) Energy loss versus frequency measured at J_p = 10 mT and J_p = 100 mT in aged samples at 100 °C (symbols and continuous lines). The bifurcation of the experimental curves beyond few MHz marks the start of the eddy current contribution in the thicker (~ 5 mm) ring sample. The dashed lines are the theoretical prediction of $W_{rot}(f)$ obtained by Eq. (1), introducing in the numerator the fitting function $\mu''_{rot}(f)$ (see Fig. 8). b) Details of the theoretical $W_{rot}(f)$ curves. The local anisotropy fields are distributed around a higher average value $\langle H_{k,eff} \rangle$ in aged samples. This brings about dramatically lower $W_{rot}(f)$ values at intermediate frequencies.

The overall broadband $W(f)$ behavior in aged and non-aged ferrites is then affected by the balance between opposite trends of the dw related quasi-static W_h and excess $W_{exc}(f)$ components and the rotation related $W_{rot}(f)$. We have shown in Figs. 2 and 3 how W_h is increased by aging and we have recognized in the induced anisotropy the main cause for this effect. On the other hand, it is quite naturally expected and actually verified in most instances that $W_{exc}(f)$ follows to some extent the destiny of W_h. Once W_h is obtained as $W_h = \lim_{f\to 0} W(f)$, the experimental $W_{exc}(f)$ is found by subtraction $W_{exc}(f) = W(f) - W_h - W_{rot}(f)$. Fig. 10 provides an illustrative example of experimental $W_{exc}(f)$ in the aged and non-aged ferrites, as obtained through the above subtraction (symbols). The chosen frequency interval is the one where $W_{exc}(f)$ can be appreciated in comparison with W_h and $W_{rot}(f)$.

It has been pointed out in previous works [13, 18] that the statistical model leading to the standard formulation for $W_{exc}(f)$ in polycrystalline steel sheets can be suitably translated to the case of sintered soft ferrites by substituting the eddy current damping coefficient $\beta_{eddy} = 4\sigma J_s^2 G\langle s\rangle$, with $G = 0.1356$ and σ the conductivity of the grain (i.e. the conductivity of the material at high frequencies) with the spin damping coefficient $\beta_{sd} = (2J_s/\mu_0\gamma\delta)\alpha$, with γ the gyromagnetic ratio, δ the dw thickness and α the damping constant. The following expression is therefore obtained

$$W_{exc}(J_p, f) = 4H_{exc}J_{p,dw} = 2V_0 n_0 \left(-1 + \sqrt{1 + \frac{4\beta_{sd} S J_{p,dw} f}{n_0^2 V_0 \langle s\rangle J_s^2}}\right) J_{p,dw} \qquad (7)$$

where H_{exc} is the so-called excess field and the statistical parameters V_0 and n_0 have the very same meaning as in magnetic steel sheets [17]. n_0 is the number of active regions (magnetic objects) concurrently reversing the magnetization under quasi-static process and V_0 is a parameter directly related to the distribution of the local coercive fields. They are obtained, for any J_p value, by simple analysis of a reduced number of experimental $W_{exc}(f)$ points. The lines fitting the experimental $W_{exc}(f)$ behaviors at $J_p = 50$ mT in Fig. 10 provide $V_0 \sim 2.8 - 17$ mA/m, increasing with aging, and $n_0 \sim 112 - 705$. Such increase of V_0 is the natural result of its direct relationship with the material coercivity.

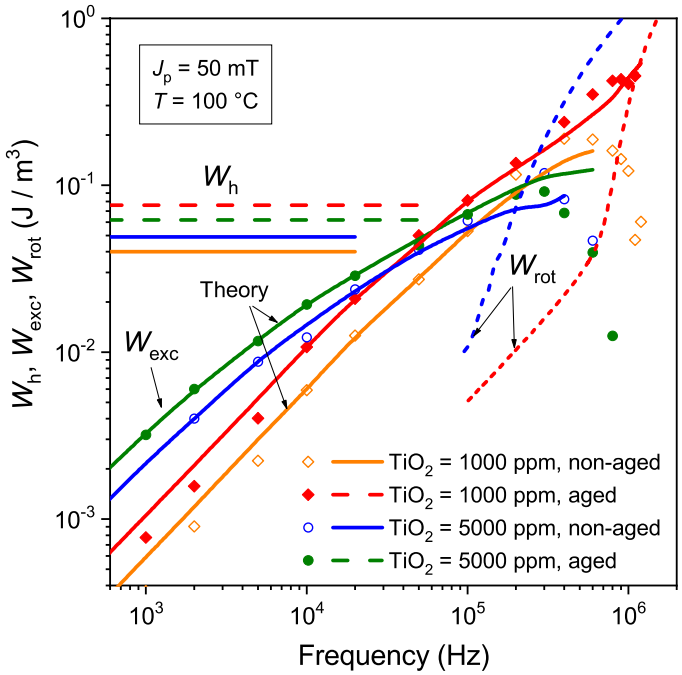

Fig. 10. The excess energy loss component $W_{exc}(f)$ (symbols) is obtained by subtracting the hysteresis W_h and the predicted rotational $W_{rot}(f)$ components from the measured loss $W(f)$. It is noted the drop of $W_{exc}(f)$ on approaching the MHz range, as expected from the observed relaxation of the dw processes. The comparison with W_h and $W_{rot}(f)$ shows that $W_{exc}(f)$ plays a role between some 50 kHz and a few hundred kHz. The fitting lines by Eq. (7) put in evidence that shielding of the induced anisotropy upon aging by the high content of TiO_2 acts in a similar way on W_h and $W_{exc}(f)$.

V. CONCLUSION

We have investigated the effect of Ti-doping on the magnetic aging performance of CoO-doped Mn-Zn ferrites. The effect of low (1000 ppm) and high (5000 ppm) TiO_2 additions on the broadband energy loss and permeability behavior before and after prolonged (100 hours) exposure at 200 °C has been assessed by separating the contributions to the magnetization process by the rotations and the dw displacements. By identifying the rotational permeability, the effective average anisotropy constant (i.e., the effective anisotropy field) is in fact determined and its increase with aging, observed at all temperatures (0 °C – 130 °C), is found to be restrained by the high-TiO_2 doping scheme. The consequences on the magnetic losses are clarified by separating the dw and rotation related contributions, according to the theoretical framework offered by the generalized Statistical Theory of Losses. The dw-associated hysteresis and the excess loss components are found to always increase upon aging, an expected detrimental outcome of the extra-anisotropy induced by the directional ordering of the Co^{2+} cations and of the dw stabilization. Such an increase is successfully limited in the high-TiO_2 ferrites, to an extent increasing with the peak polarization. It is observed, however, that at frequencies ranging between some 100 kHz and 2 MHz, aging may actually lead to a decrease of the loss, at least below some 100 mT, again to a much lower extent in the high-TiO_2 ferrites. This effect is theoretically predicted in terms of distribution of the anisotropy fields, that is, of the ferromagnetic resonance frequencies and their effect on the rotational loss component, according to the Landau-Lifshitz equation and the correspondingly calculated complex permeability.

ACKNOWLEDGMENT

This work was performed in the context of the Agreement of Scientific and Technological Cooperation between the Istituto Nazionale di Ricerca Metrologica (INRIM) and The Centre for Research and Technology Hellas (CERTH) regarding the study of soft ferrites. The work of S. Dobák was supported in part by the National Scholarship Program of the Slovak Republic.

REFERENCES

[1] H. Shokrollahi and K. Janghorban, Influence of additives on the magnetic properties, microstructure and densification of Mn-Zn soft ferrites, Mater. Sci. Eng. B 141 (2007) 91-107, doi: 10.1016/j.mseb.2007.06.005.

[2] A. Znidarsic, M. Limpel, and M. Drofenik, Effect of dopants on the magnetic properties of MnZn ferrites for high frequency power supplies, IEEE Trans. Magn. 31 (1995) 950–953, doi: 10.1109/20.364767.

[3] S. Wang, Y. Chiang, Y. Hsu, and C. Chen, Effects of additives on the loss characteristics of Mn-Zn ferrite, J. Magn. Magn. Mater. 365 (2014) 119-125, doi: 10.1016/j.jmmm.2014.04.043.

[4] A.D. Giles and F.F. Westendorp , The effect of cobalt substitutions on some properties of manganese zinc ferrites, J. Phys. D: Appl. Phys. 9 (1976) 2117-2122, doi: 10.1088/0022-3727/9/14/020.

[5] A. Fujita and S. Gotoh, Temperature dependence of core loss in Co-substituted MnZn ferrites, J. Appl. Phys. 93 (2003) 7477-7479, doi: 10.1063/1.1557952.

[6] L. Li, Z. Lan, Z. Yu, K. Sun, and Z. Xu, Effects of Co-substitution on wide temperature ranging characteristic of electromagnetic properties in MnZn ferrites, J. Alloys Comp. 476 (2009) 755-759, doi: 10.1016/j.jallcom.2008.09.101.

[7] K. Mori, K. Yasuhara, I. Nakahata, and K. Nishikawa, High temperature stability of Co-doped MnZn ferrites for automobiles, *J. Jpn. Soc. Powder Powder Metallurgy*, 61 (2014) S224-S226, doi: 10.2497/jjspm.61.S224.

[8] C. Beatrice, S. Dobák, V. Tsakaloudi, C. Ragusa, F. Fiorillo, L. Martino, and V. Zaspalis, Magnetic loss, permeability, and anisotropy compensation in CoO-doped Mn-Zn ferrites," AIP Adv. 8 (2018) 047803, doi: 10.1063/1.4993718.

[9] S. Dobák, C. Beatrice, F. Fiorillo, V. Tsakaloudi, and C. Ragusa, Magnetic loss decomposition in Co-doped Mn-Zn ferrites, IEEE Magn. Lett. 10 (2019) 7100205, doi; 10.1109/LMAG.2018.2881108

[10] A. Giles and F. Westendorp, Simultaneous substitution of cobalt and titanium in linear manganese zinc ferrites, J. Phys. (France) 38-C1 (1977) 47-50, doi: 10.1051/jphyscol:1977109.

[11] V. T. Zaspalis and E. Eleftheriou, The effect of TiO_2 on the magnetic power losses and electrical resistivity of polycrystalline MnZn ferrites, J. Phys. D *38* (2005) 2156–2161, doi: 10.1088/0022-3727/38/13/012.

[12] A. Yanase, Mechanism of disaccommodation in ferrite, J. Phys. Soc. Japan 6 (1962) 1005-1011, doi: 10.1143/JPSJ.17.1005.

[13] E. Ferrara, F. Fiorillo, C. Beatrice, S. Dobák, C. Ragusa, A. Magni, and C. Appino, Characterization and assessment of the wideband magnetic properties of nanocrystalline alloys and soft ferrites, J. Mater. Res. 33, (2018) 2120-2137, doi: 10.1557/jmr.2018.275.

[14] F. Fiorillo and C. Beatrice, A comprehensive approach to broadband characterization of soft ferrites, Int. J. Appl. Electromagn. Mech. 48 (2015) 283–294, doi: 10.3233/JAE-152000.

[15] B. Sun, F. Chen, W. Yang, H. Shen, and D. Xie, Effects of nano-TiO_2 and normal size TiO_2 additions on the microstructure and magnetic properties of manganese-zinc power ferrites, J. Magn. Magn. Mater. 349 (2014) 180-187, doi: 10.1016/j.jmmm.2013.09.006.

[16] C. Beatrice, V. Tsakaloudi, S. Dobák, V. Zaspalis, and F. Fiorillo, Magnetic losses versus sintering treatment in Mn-Zn ferrites," J. Magn. Magn. Mater. 429 (2017) 129-137, doi: 10.1016/j.jmmm.2016.12.121.

[17] G. Bertotti, *Hysteresis in Magnetism* (Academic Press, San Diego, CA, USA, 1998), p. 411.

[18] F. Fiorillo, C. Beatrice, O. Bottauscio, M. Chiampi, and A. Manzin, An approach to magnetic losses and their frequency dependence in Mn-Zn ferrites, Appl. Phys. Lett. 89 (2006), 122513, doi: 10.1063/1.2356111.